STRUCTURAL CHEMISTRY

ISSN: 2053-2296
journals.iucr.org/c

Synthesis, crystal structure and study of the crystal packing in the complex bis(4-aminopyridine-κN^1)dichloridocobalt(II)

Olga Carolina Sanchez Montilva, Federico Movilla, Maricel Gabriela Rodriguez and Florencia Di Salvo

Acta Cryst. (2017). C**73**, 399–406

Acta Cryst C STRUCTURAL CHEMISTRY
ISSN 2053-2296

Synthesis, crystal structure and study of the crystal packing in the complex bis(4-aminopyridine-κN^1)-dichloridocobalt(II)

Olga Carolina Sanchez Montilva, Federico Movilla, Maricel Gabriela Rodriguez and Florencia Di Salvo*

Departamento de Química Inorgánica, Analítica y Química Física/INQUIMAE–CONICET, Facultad de Ciencias Exactas y Naturales, Universidad de Buenos Aires, Intendente Güiraldes 2160, Buenos Aires, Argentina. *Correspondence e-mail: flor@qi.fcen.uba.ar

Received 12 September 2016
Accepted 29 March 2017

Edited by Y. Ohgo, Teikyo University, Japan

Keywords: cobalt complex; 4-aminopyridine; pyridine–pyridine dimer; crystal structure; π–π stacking; Hirshfeld analysis; fingerprint plots.

CCDC reference: 1540857

Supporting information: this article has supporting information at journals.iucr.org/c

Despite the large number of reported crystalline structures of coordination complexes bearing pyridines as ligands, the relevance of π–π interactions among these hereroaromatic systems in the stabilization of their supramolecular structures and properties is not very well documented in the recent literature. The title compound, $[CoCl_2(C_5H_6N_2)_2]$, was obtained as bright-blue crystals suitable for single-crystal X-ray diffraction analysis from the reaction of 4-aminopyridine with cobalt(II) chloride in ethanol. The new complex was fully characterized by a variety of spectroscopic techniques and single-crystal X-ray diffraction. The crystal structure showed a tetrahedral complex stabilized mainly by bidimensional motifs constructed by π–π interactions with large horizontal displacements between the 4-aminopyridine units, and N—H···Cl hydrogen bonds. Other short contacts, such as C—H···Cl interactions, complete the three-dimensional arrangement. The supramolecular investigation was extended by statistical studies using the Cambridge Structural Database and a Hirshfeld surface analysis.

1. Introduction

The structural characteristics of pyridine-based cobalt(II) complexes have been widely studied in the literature for some time (Gill & Nyholm, 1961; Clarke & Milledge, 1975; Brown, 1985). Depending on the nature of the pyridine ligand and the total number of coligands, the cobalt ion can assume an octahedral or a tetrahedral environment (Jian *et al.*, 2008, and references therein). In particular, materials composed of $CoCl_2L_2$, with L denoting a pyridine ring (py), have shown a wide variety of applications, ranging from gas storage in porous frameworks to novel luminescent or magnetic applications (Teo & Hor, 2011; Sun *et al.*, 2010; Steed & Atwood, 2009; Férey, 2008; Chi & Chou, 2007; Robin & Fromm, 2006). On the other hand, it is expected also that the geometry of the complex, the presence of the π-system itself and the nature of the substituent on the pyridine ring will play an important role in the crystal packing due to the presence of different types of intermolecular contacts, such as π–π interactions, dispersive interactions and hydrogen bonds, among others.

Noncovalent interactions in nitrogen-containing heterocycles, including aromatic–aromatic stacking interactions, have been intensively studied because of their importance in numerous systems, from biomolecules to molecular crystals. Aromatic interactions using two benzene molecules as models have been extensively studied from the theoretical point of view, but there have only been a small number of structural

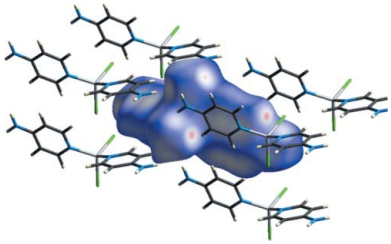

studies on pyridine dimers. The effect of heteroatoms on π–π interactions have been evaluated recently *via* high-level quantum chemical computational methods (Smith & Gordon, 2011; Wheeler, 2011) and experimental structure analysis using the Cambridge Structural Database (CSD; Groom *et al.*, 2016), providing a better understanding of the nature and relevance of these kinds of interactions among pyridine-based systems. The presence of a heteroatom reduces the spatial extent of the π-electron cloud and the polarizability of pyridine as compared to benzene. As a result, the magnitude of the dispersion, exchange and induction interactions in benzene–pyridine and pyridine–pyridine dimers are generally reduced compared to those for the benzene–benzene dimer. As a consequence, benzene–pyridine and pyridine–pyridine dimers bind more strongly than the benzene–benzene dimer in several configurations and, in contrast to the benzene–benzene dimer, parallel-displaced configurations (offset) can be significantly preferred over T-shaped configurations (Nincovic *et al.*, 2013).

Hydrogen bonding can generate a diverse array of architectures through self-assembly in supramolecular transition metal chemistry (Wang *et al.*, 2016; Hardy, 2013). The most popular ligands are those bearing N-donor atoms and additional polar functionalities capable of giving rise to strong hydrogen bonding. In the absence of strong acceptors, other atoms, such as halogens, can participate in hydrogen bonding, with a considerable relative decrease of the interaction strength (Bujak, 2015; Bacchi *et al.*, 2014).

Despite the considerable amount of reported crystal structures of coordination complexes bearing pyridines as ligands, the relevance of π–π interactions among these heteroaromatic systems in the stabilization of their supramolecular structures and properties is not very well documented in the recent literature. As a contribution to this field, we report herein the synthesis, crystal structure and supramolecular analysis of a new cobalt(II) complex, $CoCl_2$(4-aminopyridine)$_2$, (I), highlighting the role of π–π interactions in the structural packing, together with the other intermolecular interactions present in the system. To complete our supramolecular analysis, Hirshfeld surface (HS) studies (Hirshfeld, 1977) and Cambridge Structural Database (CSD, Version 5.34; Groom *et al.*, 2016) investigations are also performed.

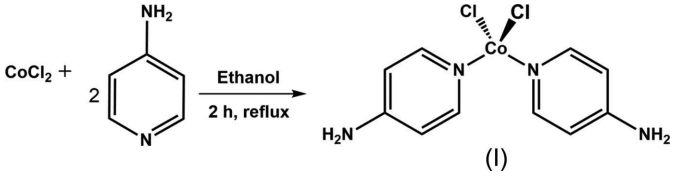

(I)

2. Experimental

2.1. General

Chemicals were obtained and used as follows: ethanol was distilled from CaH_2 and $CoCl_2{\cdot}6H_2O$ (98.9%, Fluka) and 4-aminopyridine (97% Aldrich) were used as received. FT–IR spectra were recorded from a KBr pellet on a Thermo Nicolet FT–IR AVATAR 320 spectrometer. The UV–Vis spectra were recorded on a Hewlett Packard 8453 diode array spectrometer equipped with a Lauda RE 207 thermostat using a screw-capped quartz cuvette. The ^{1}H NMR spectrum was recorded on a Bruker AVANCE II 500 MHz spectrometer and referenced to the solvent (^{1}H, residual d_6-acetone). Chemical shifts (δ) are reported in ppm and coupling constants (J) in Hz; peaks are described as follows: *s* = singlet, *d* = doublet, *t* = triplet, *sept* = septet, *br* = broad and *m* = multiplet. Elemental analyses (C, H and N) were performed on a Carlo Erba CHNS EA-1108 microanalyzer.

Table 1
Experimental details.

Crystal data	
Chemical formula	$[CoCl_2(C_5H_6N_2)_2]$
M_r	316.98
Crystal system, space group	Monoclinic, *C*2/*c*
Temperature (K)	293
a, *b*, *c* (Å)	8.9262 (9), 9.9679 (10), 14.9683 (13)
β (°)	101.825 (10)
V (Å^3)	1303.6 (2)
Z	4
Radiation type	Mo $K\alpha$
μ (mm^{-1})	1.66
Crystal size (mm)	0.63 × 0.12 × 0.05
Data collection	
Diffractometer	Agilent Xcalibur Gemini Eos with CCD plate detector
Absorption correction	Multi-scan (*CrysAlis PRO*; Agilent, 2013)
T_{min}, T_{max}	0.349, 1.000
No. of measured, independent and observed [$I > 2\sigma(I)$] reflections	4351, 1515, 790
R_{int}	0.099
(sin $\theta/\lambda)_{max}$ (Å^{-1})	0.678
Refinement	
$R[F^2 > 2\sigma(F^2)]$, $wR(F^2)$, S	0.062, 0.143, 1.01
No. of reflections	1515
No. of parameters	81
H-atom treatment	H atoms treated by a mixture of independent and constrained refinement
$\Delta\rho_{max}$, $\Delta\rho_{min}$ (e Å^{-3})	0.48, −0.37

Computer programs: *CrysAlis PRO* (Agilent, 2013), *SHELXS97* (Sheldrick, 2008), *SHELXL2014* (Sheldrick, 2015), *OLEX2* (Dolomanov *et al.*, 2009) and *PLATON* (Spek, 2009).

2.2. Synthesis and crystallization

To a solution of cobalt(II) chloride dihydrate (100 mg, 0.77 mmol) in ethanol was added 4-aminopyridine (144.76 mg, 1.54 mmol) under an N_2 atmosphere and the mixture was stirred under reflux for 2 h (see Scheme 1). After cooling the mixture to room temperature, the crystalline solid was removed by filtration under vacuum. The compound was obtained as bright-blue crystals (yield 60.5%) of suitable quality for single-crystal X-ray diffraction studies. ^{1}H NMR (500 MHz): δ 2.78–2.26 (*s*, 4H), 41.16–38.55 (*s*, 4H), 163.95–152.36 (*s*, 4H). FT–IR (in cm^{-1}): ν_{NH} = 3440 and 3340, ν_{CH} ∼ 3200, ν_{NH} ∼ 1630, ν_{CC} ∼ 1630. UV–Vis (λ in nm): in acetone

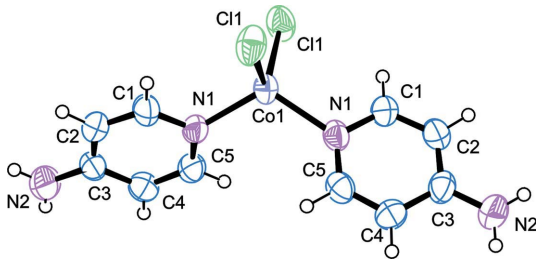

Figure 1
The molecular structure of $CoCl_2$(4-aminopyridine)$_2$, (I), showing the atomic numbering scheme.

(6.9×10^{-4} *M*), 577 (ε = 647 M^{-1} cm^{-1}), 612 (ε = 1014 M^{-1} cm^{-1}), 626 (ε = 1054 M^{-1} cm^{-1}). For more details, see the *Supporting information*.

2.3. Single-crystal XRD measurement and refinement

Crystal data, data collection and structure refinement details are summarized in Table 1. All H atoms were placed in idealized positions and refined in riding modes such that U_{iso}(H) = 0.06U_{eq}(parent).

2.4. Searching in the Cambridge Structural Database (CSD)

For the statistical molecular analysis, a CSD (Version 5.34; Groom *et al.*, 2016) search was carried out with the program *ConQuest* (Version 1.18; Bruno *et al.*, 2002). The intramolecular parameters of the reported structure were compared with those of similar molecules deposited in the CSD using the *Mogul* program (Bruno *et al.*, 2005). The search was performed using the following criteria: (i) crystallographic *R* factor < 10%, (ii) no disordered structures, (iii) structures resolved from powder data not included and (iv) normalized H-atom positions with CSD criteria. Additionally, in order to study the π–π interactions throughout systems bearing coordinated pyridine rings, the model described in Fig. S2 (see *Supporting information*) was used to run the search in the CSD. The centre-to-centre distance (distance between ring centroids, CCD) was restricted in the range 0.1–6 Å and the angle between the two planes containing the moieties was fixed at < 10° (parallel orientation criteria).

3. Results and discussion

3.1. Molecular structure

The title Co^{II} compound was synthesized according to adapted procedures (Jian *et al.*, 2008) and was obtained in a reasonable yield. Its purity was demonstrated using different characterization techniques. Despite the paramagnetic nature of the metal ion, NMR studies were supportive of the identity of the organic ligands. As mentioned in the *Experimental* section, the complex was obtained as a crystalline material of quality suitable for analysis by single-crystal X-ray diffraction. The structural results show an asymmetric unit that consists of a tetracoordinated cobalt(II) ion bearing two N atoms from two 4-aminopyridine ligands and two chloride ligands (Fig. 1), with angles of 109.68 (9), 116.6 (2), 107.96 (13) and

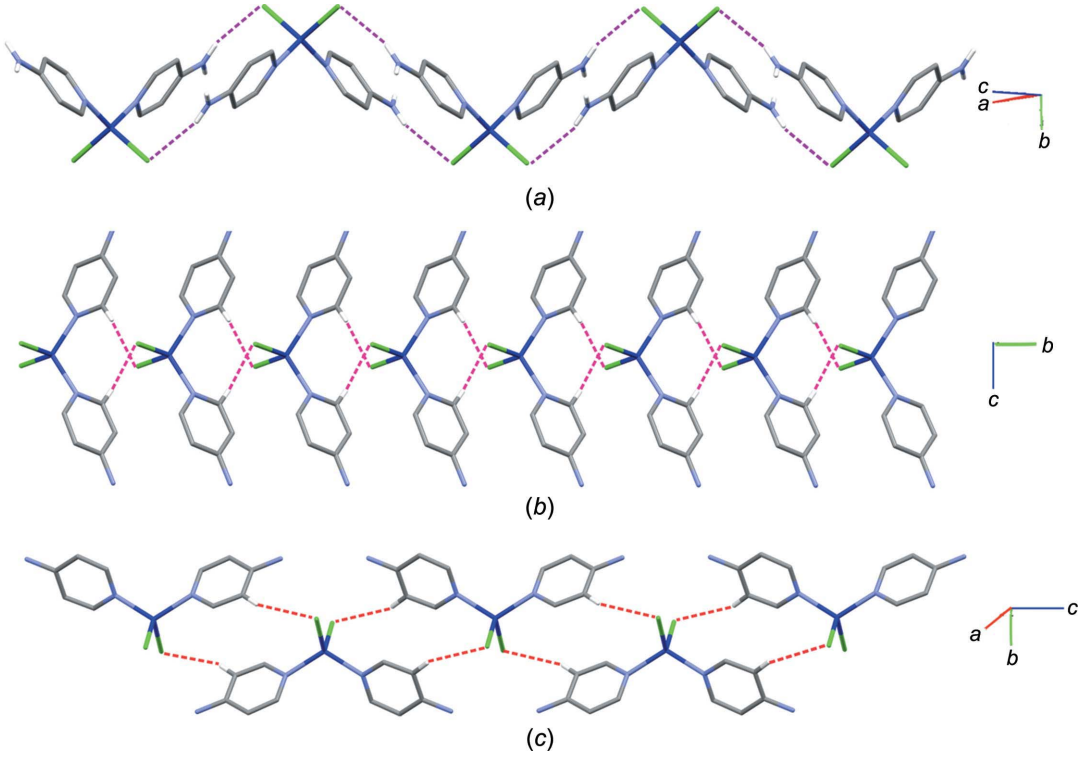

Figure 2
Intermolecular interactions of $CoCl_2$(4-aminopyridine)$_2$, (I), showing (*a*) N2—H2b···Cl (violet dashed line), (*b*) C5—H5···Cl (magenta dashed line) and (*c*) C2—H2···Cl (red dashed line). H atoms not involved in the short contacts have been omitted for clarity.

107.29 (13)° for Cl—Co—Cl^{i}, N—Co—N^{i}, N—Co—Cl and N—Co—Cl^{i}, respectively [symmetry code: (i) $-x+1, y, -z+\frac{3}{2}$]. The bond lengths are 2.006 (4) Å for Co—N and 2.2652 (15) Å for Co—Cl. The main geometrical parameters are given in Table S1 of the *Supporting information*. The visible spectrum in solution presents absorption bands in agreement with a tetrahedral Co^{II} complex, indicating the same complex exists in solution as in the solid state (Fig. S3 of the *Supporting information*). For tetrahedral Co^{II} coordination compounds, the absorbance observed in the visible region corresponds to the high-energy electronic transition ν_3, $^4A_2 \rightarrow {}^4T_1$(P). When the symmetry of a tetrahedral compound is lowered, the orbital triplet level, T_1, splits into three energy levels, producing additional peaks in the spectrum, as observed for (I). Thus, the degree of splitting in the visible transition could be interpreted as arising from a certain degree of distortion from an idealized tetrahedral structure (*e.g.* angles deviating from 109.5°; Lever, 1968).

In order to compare the intramolecular parameters of (I), a search of the CSD was performed using one pyridine or one 4-NX_2-pyridine (X = H and C) and one Cl atom, both coordinated to any transition metal as queries and considering a tetracoordinated metal ion. The results showed 3158 hits for the pyridine and among them just 32 corresponded to 4-amino-subtituted pyridines. In order to evaluate the Cl—M—Cl and N—M—N angles, the searches were run using two chlorides and one pyridine or one 4-NX_2-pyridine and *vice versa* (see the *Supporting information*). The histogram plots considering the most relevant structural parameters of the searches are shown in the *Supporting information* with the values for (I) indicated in the corresponding figures (Figs. S4 and S5). It was found that all the bond lengths of (I) are in agreement with the expected values considering they lie in the observed ranges and are near the average of each analysed criterion. For the angles, the same behaviour is observed considering only the portion of the histograms that corresponds to the tetrahedral geometry. Due to the angles not being restricted in the searches, both geometries, *i.e.* tetrahedral and square planar, are observed in the same plot. On the other hand, of the 32 complexes, only two correspond to closely related structures, namely dichloridobis[4-(dimethylamino)pyridine]cobalt(II) (CSD refcode DODNUG; Jian *et al.*, 2008) and bis(4-amino-2-chloropyridine)dichloridozinc(II) (CSD refcode RIRKUZ; Zhou *et al.*, 2007). A comparative supramolecular analysis is outlined below.

3.2. Supramolecular structure

The supramolecular analysis of (I) shows a packing arrangement constructed by face-to-face π-stacking with a large horizontal displacement (offset) exhibited by the aminopyridine dimers, and adjacent N—H···Cl hydrogen bonds (Tables 2 and 3, and Fig. 2). The N—H···Cl interactions give rise to infinite chains oriented along the crystallographic *ac* plane (Fig. 2*a*). Associated with these hydrogen bonds, hexagonal motifs lying in the crystallographic *ab* plane constructed by π–π interactions between three 4-amino-pyridine dimers are observed (Fig. 3). In the hexagonal embrace, each pair of interacting π-systems shows a different orientation; nevertheless, all of them display similar structural features (Table 3 and Fig. 4). For both benzene–benzene and pyridine–pyridine parallel interactions, the most frequent geometries in the CSD are at large offsets (above 4.5 Å) and not at distances of 1.5–2.0 Å, which correspond to a parallel-like geometry (Nincovic *et al.*, 2013). In consequence, all three observed 4-aminopyridine–4-aminopyridine dimers exhibited in (I) could be considered strong enough to be indicated as essential for the crystal packing. As reported, due to the electron-withdrawing effect exerted by the Co^{II} ion, it is expected that heterocycles like the pyridine ligand is well suited for π–π interactions because of its low π-electron density (Janiak, 2000). The significance of noncovalent interactions among pyridine rings has been the object of recent studies due to the biological relevance and also due to the fact that benzene–pyridine and pyridine–pyridine dimers bind more strongly than the benzene–benzene dimer in several configurations (Nincovic *et al.*, 2013). Thus, we find that complex (I) is a good example where the interactions exhibited by the pyridine rings have an important role in the crystal packing. Finally, the three-dimensional supramolecular network is completed by nonconventional C—H···Cl hydrogen bonds between the C2 and C5 H atoms and the chloride ligands (Figs. 2*b* and 2*c*).

Table 2
Hydrogen-bond geometry (Å, °) for complex (I).

D—H···A	D—H	H···A	D···A	D—H···A
C5—H5···Cl1^{i}	0.93 (1)	2.930 (6)	3.644 (6)	176 (1)
C2—H2···Cl1^{ii}	0.93 (1)	2.869 (6)	3.727 (6)	154 (1)
N2—H2b···Cl1^{iii}	0.86 (1)	2.615 (6)	3.447 (6)	163 (1)

Symmetry codes: (i) $-x+\frac{1}{2}, y+\frac{1}{2}, -z+\frac{3}{2}$; (ii) $-x+1, -y+1, -z+1$; (iii) $-x+\frac{1}{2}, -y+\frac{3}{2}, -z+1$.

Table 3
Different π–π interactionsin the structure of (I).

*Cg*1 is the centroid of pyridine ring, CCD is the centre-to-centre distance (distance between ring centroids), DA is the dihedral angle, SA is the slippage angle (angle subtended by the intercentroid vector to the plane normal), IPD is the interplanar distance (distance from one plane to the neighbouring centroid) and R is the normal distance between the planes of the interacting rings.

Dimer	Ring 1···Ring 2	CCD (Å)	R (Å)	DA (°)	SA (°)	IPD (Å)
A	*Cg*1···*Cg*1^{iv}	4.523 (4)	3.377 (5)	0.03	41.70	3.009
B	*Cg*1···*Cg*1^{v}	4.833 (4)	3.098 (5)	0.00	50.12	3.326
C	*Cg*1···*Cg*1^{vi}	4.924 (4)	3.057 (5)	0.00	51.60	3.976

Symmetry codes: (iv) $-x+1, -y+1, -z+1$; (v) $-x+\frac{1}{2}, -y+\frac{3}{2}, -z+1$; (vi) $-x+\frac{3}{2}, -y+\frac{3}{2}, -z+1$.

3.2.1. Crystallographic database studies. As mentioned previously, according to the CSD, there is a vast number of reported crystal structures of coordination complexes bearing pyridine as ligands and, among them, 49185 (77%) present pyridine–pyridine interactions. A CCD (distance between ring centroids) value < 6 Å was used as the criterion to find the crystal structures showing π-stacking among the heteroaro-

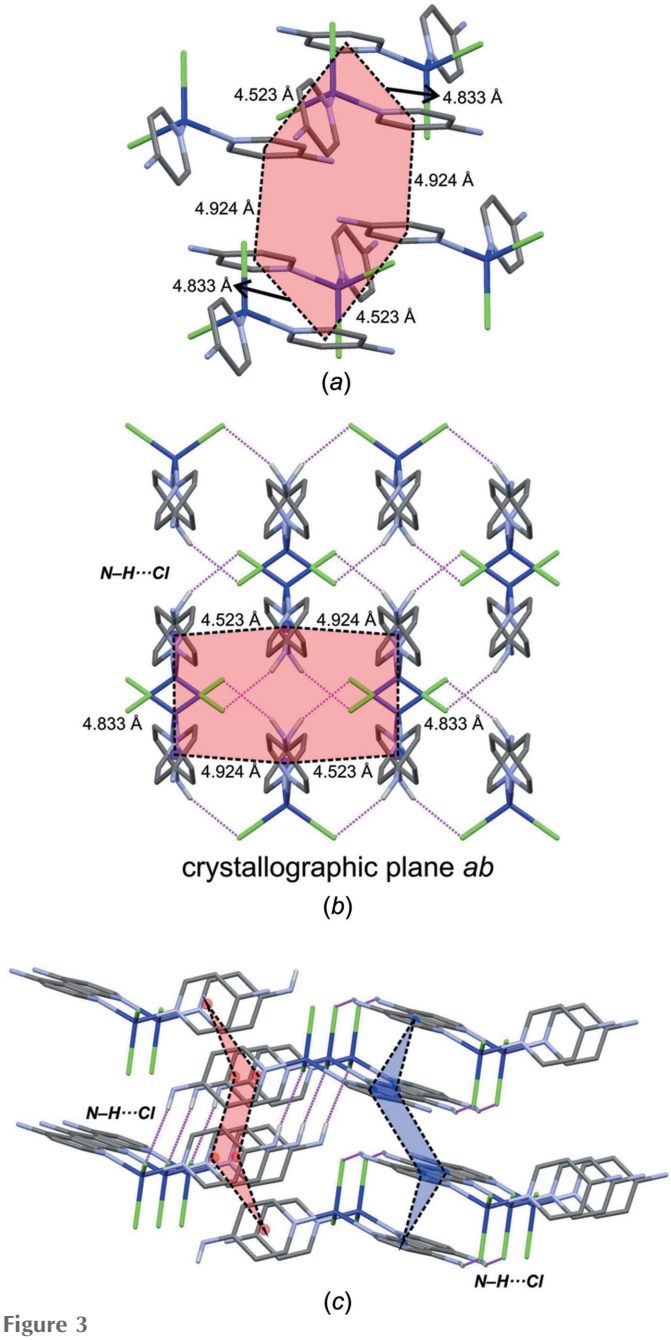

Figure 3
Hexagonal motifs described by π–π interactions in 4-aminopyridine dimers, showing (*a*)/(*c*) a random orientation for visualization, and (*b*) a view along the crystallographic *ab* plane. In part (*c*), two hexagonal arrangements belonging to two different corrugated planes are described. N—H···Cl hydrogen bonds are shown with pink dashed lines. H atoms not involved in the short contacts have been omitted for clarity.

matic rings (Fig. S2 in the *Supporting information*), a value used in previously reported work. A large number of hits and a similar relative proportion of crystals bearing pyridine–pyridine interactions is also observed when the search is run using pyridine—*M*—Cl as the search fragment (8146 hits, 76%) (*M* is any transition metal). The number is reduced significantly when tetraccordinated metals are considered, but the relative proportion does not change (2382 hits, 75%). A different behaviour is observed when the substituent is taken

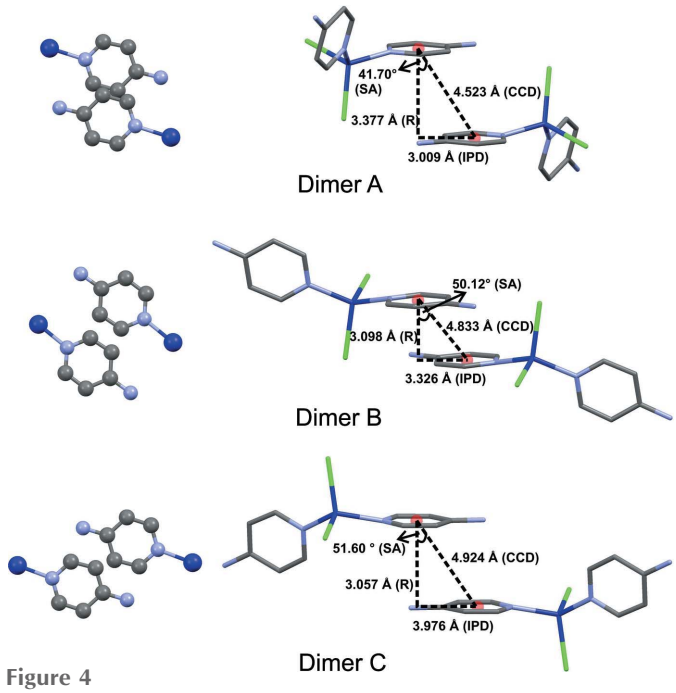

Figure 4
π–π stacking in 4-aminopyridine dimers (**A**, **B** and **C**) depicting three different orientations.

Table 4
Structural comparison (Å) of different aminopyridine–metal complexes.

Compound	Interactions			
	N—H···Cl	C—H···Cl	Cl···Cl	π–π
$CoCl_2$(4-aminopyridine)$_2$, (I)	2.615	2.869/2.930		4.523
$CoCl_2$[4-(dimethylamino)pyridine]$_2$		2.789/2.825		
$ZnCl_2$(4-amino-2-chloropyridine)$_2$	2.928	2.711	3.371	

into account in the ring, *i.e.* when 4-NX_2-pyridine—*M*—Cl is used to perform the search, only 46 structures that show this short contact are obtained and represent 53% of the total number of hits. As expected, this number decreases when only four-coordinated complexes are considered, with just 19 crystal structures (59% of the total number of hits) exhibiting π–π interactions between pyridine rings in their supramolecular structures. This difference could be associated with the steric effect exerted by the substituent and also shows that although this kind of interaction was found in many structures reported at the CSD, it does not seem to be common among aminopyridine–metal complexes. The complex dichloridobis{3,3′-[(pyridin-4-yl)imino]dipropanenitrile}cobalt(II) (CSD refcode XINZOL; Ni *et al.*, 2013) illustrates this concept, where the absence of pyridine–pyridine short contacts could be attributed to the bulkiness of the propylacetonitrile substituents (Fig. S6 in the *Supporting information*). A statistical analysis of the pyridine–pyridine interactions considering these searches is shown in Fig. S7 of the *Supporting information*. As already mentioned, the three 4-aminopyridine–4-aminopyridine dimers observed in (I) show CCD distances that are in agreement with the observed values in the CSD (Fig. S7 in the *Supporting information*).

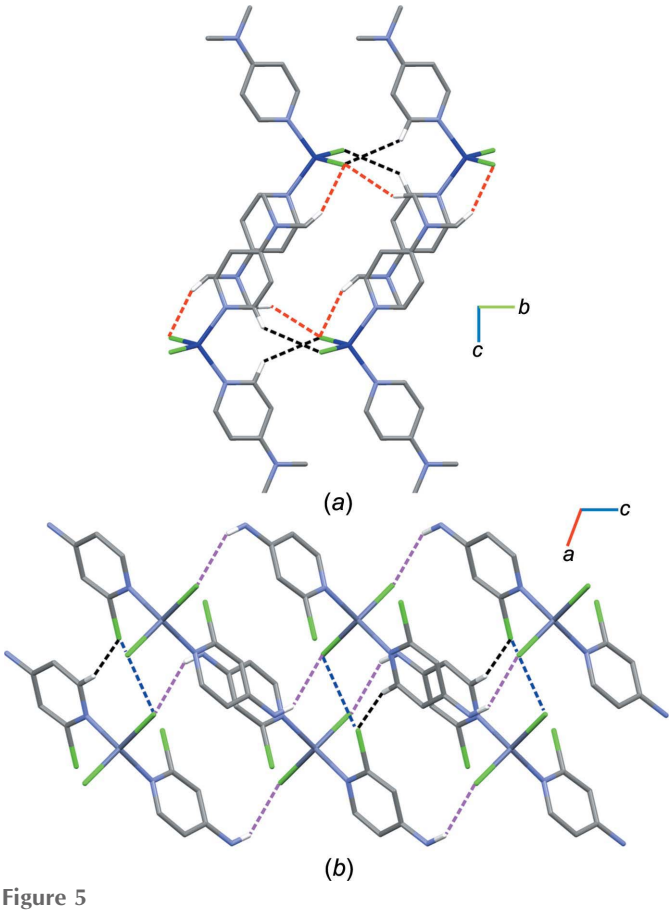

Figure 5
The packing arrangement of aminopyridine–metal complexes related to $CoCl_2$(4-aminopyridine)$_2$, (I), showing (*a*) dichloridobis[4-(dimethylamino)pyridine]cobalt(II) and (*b*) bis(4-amino-2-chloropyridine)dichloridozinc(II). The contacts shown are N—H···Cl (magenta dashed lines), (CH_3)C—H···Cl (red dashed lines), (pyridine)C—H···Cl (black dashed lines) and Cl···Cl (blue dashed lines). H atoms not involved in short contacts have been omitted for clarity.

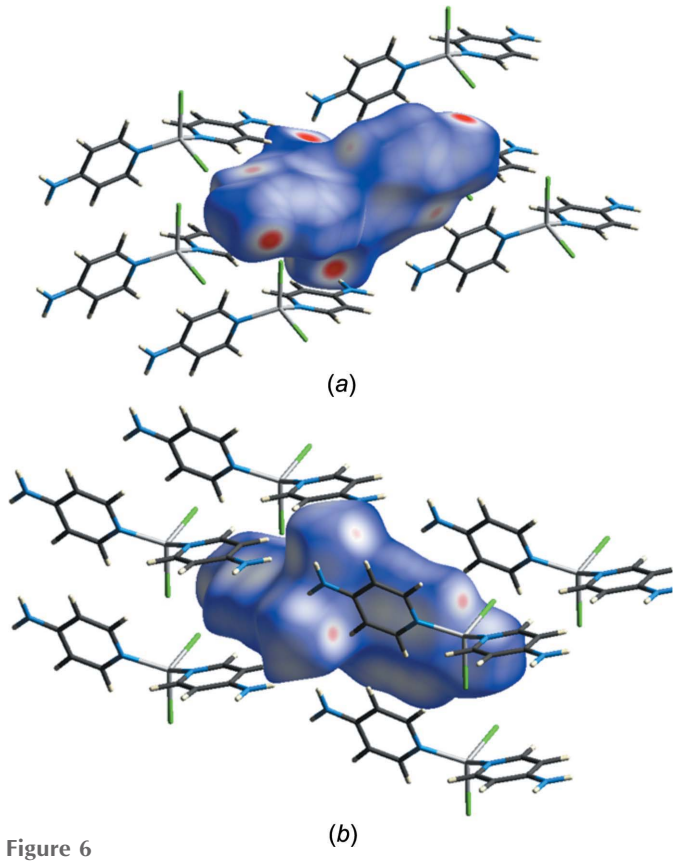

Figure 6
(*a*) Front view and (*b*) back view of the HS including the neighbouring molecules associated with the closer contacts.

As mentioned previously, we found only two structures in the CSD closely related to (I), namely $CoCl_2$[4-(dimethylamino)pyridine]$_2$ (CSD refcode DODNUG; Jian *et al.*, 2008) and $ZnCl_2$(4-amino-2-chloropyridine)$_2$ (CSD refcode RIRKUZ; Zhou *et al.*, 2007) (Fig. S6 in the *Supporting information*). Although the compounds have structural similarities, π-stacking interactions are present only in (I), probably as a result of the orientation of the 4-aminopyridine rings and the assistance of the N—H···Cl hydrogen bonds (see Table 4 and Fig. 5). In the other two structures, the crystal packing exhibits very long displacements between the aminopyridine rings (6.499 and 7.69 Å, respectively), with distances beyond what it is considered valid for such interactions (see above). Therefore, the rings do not face each other completely, resulting in the absence of interactions. It is interesting to point out that not only the presence of methyl groups in the amine substitutent but also the substitution of the pyridine ring in another position influences the π-interaction. On the other hand, C—H···Cl contacts are observed for both structures as well, with distances in the range 2.711–2.930 Å. Other differences between (I) and $CoCl_2$[4-(dimethylamino)pyridine]$_2$ lie in the supramolecular arrangement described by the N—H···Cl interactions, which are not present in the second compound due to the methyl groups. In the Zn^{II} complex, infinite chains sustained by N—H···Cl hydrogen bonds are observed along the crystallographic *a* axis. It is important to mention that $ZnCl_2$(4-amino-2-chloropyridine)$_2$ is the only one of the three complexes which exhibits Cl···Cl close contacts involving the Cl atom of the aminopyridine ring. The stronger nature of the halogen contacts presumably precludes the existence of π-interactions involving the heteroaromatic rings (Table 4).

3.2.2. Hirshfeld surface generation and fingerprint plot analysis. Hirshfeld surface (HS) analysis is a valuable method for the analysis of intermolecular contacts that offers a whole-molecule approach. Thus, a HS analysis has been performed for (I) using the program *Crystal Explorer* (Spackman & Jayatilaka, 2009), considering standard neutron diffraction values for the bond distance involving H atoms (C—H = 1.083 Å, O—H = 0.983 Å and N—H = 1.015 Å). The information given by the HS analysis agrees fully with the supramolecular investigation described above. In the HS plots shown in Fig. 6, the intense red dots represent the C5—H5···Cl1^{i}, C2—H2···Cl1^{ii} and N2—H2b···Cl1^{iii} interactions (Table 2) and the light-red dots observed on atom C2 of the heteroaromatic ring indicate the nearest contact portion of the π–π interaction among 4-aminopyridine dimers. In order to investigate closely the π–π interactions described previously,

the mappings around the 4-aminopyridine ligands were analysed carefully (Fig. 6). Of the three different dimers, that having the shortest R distance (normal distance between the planes of the interacting rings), represented in Fig. 4(*c*), is easily recognized and confirmed by HS analysis as relevant in the crystal packing (Fig. 7). Although the other two dimers can be identified as pairs of 4-aminopyridine ligands interacting through π-stacking based on previously reported work and CSD statistical studies, only one of them is confirmed using the d_{norm} mapped on the HS (Fig. 7*c* and Fig. S8 in the *Supporting information*). Besides, the confirmation denoted by the existence of the red dots in both interacting molecules is only observed for dimer **C** and not for the others (Fig. S8 in the *Supporting information*). Although in all of them the π–π interaction seems to be a consequence of the associated hydrogen bond, in dimers **A** and **B**, as indicated in Fig. 7, the interaction involving the rings can hardly be regarded as a relevant interaction in comparison with dimer **C**.

The fingerprint plots (2D-FP) generated by the HS analysis (Spackman & McKinnon, 2002) represent a very simple way of determining the full distribution of the interactions exhibited in the crystal (Fig. 8). These plots show the frequency of occurrence of the main interactions represented by coloured bright areas depending on the intensity: blue (low), green (medium) and red (high). Also, to identify the portion of the surface where a complementary interaction between two molecules take place, with one molecule acting as donor and the other as acceptor, the reciprocal contacts contributing to an individual $X\cdots Y$ interaction can be plotted. The 2D-FP plots of (I) are depicted in Fig. 8 and, as expected and already discussed, the Cl$\cdots$H and C$\cdots$H interactions are very important over all the surface area (31.6 and 21.8%, respectively). On the other hand, the remaining hydrogen bond represented by the N$\cdots$H interaction, does not contribute considerably to the crystal packing. This result could probably be explained by the long intermolecular displacement between the N atom of the amine and a H atom of the adjacent amino group. The H$\cdots$H contacts comprise 36% of the total HS area which could be associated with the interaction between two organic ligands, *i.e.* the 4-aminopyridine–4-aminopyridine dimers. This analysis shows again the relevance of π-interactions in the crystal packing. As a final observation, it interesting to note that the shape index function graph shows intense red zones in concordance with the position and orientation of the contact observed in the Hirshfield d_{norm} surface, denoting a good complementarity between molecules in the unit cell and also a close compact arrangement (Figs. 6–8).

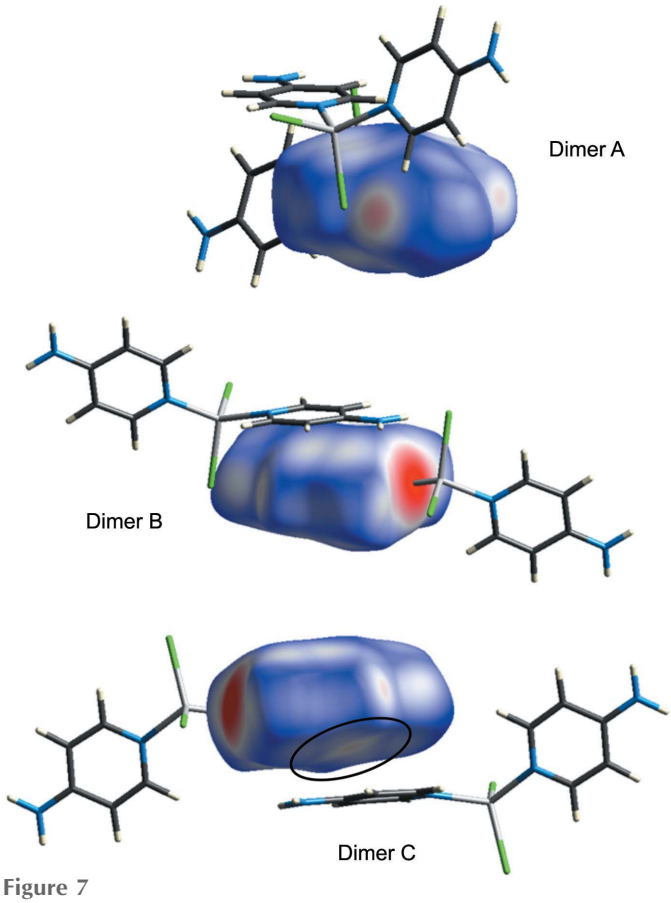

Figure 7
Portions of the HS of the three 4-aminopyridine–4-aminopyridine dimers, showing π–π contacts (see Fig. 4 for reference). Notice that dimer **A** is rotated with respect to Fig. 4 in order to observe the interaction more clearly and in dimer **C**, unlike in dimers **A** and **B**, the interaction is represented by a very weak red dot highlighted with a black circle.

4. Conclusions

A new Co^{II}–aminopyridine complex, $CoCl_2$(4-aminopyridine)$_2$, has been synthesized and characterized using single-crystal X-ray diffraction analysis and other spectroscopic techniques. The crystal packing in $CoCl_2$(4-aminopyridine)$_2$ is driven by π–π interactions between 4-aminopyridine dimers and N—H$\cdots$Cl hydrogen bonds and other less relevant noncovalent interactions, such as C—H$\cdots$Cl. Its structural and supramolecular features were compared with the results obtained from CSD searches, finding that both molecular and intermolecular parameters are in agreement with similar reported structures. Although there is an enormous number of reported crystal structures of coordination compounds bearing pyridines as ligands, the number of examples exhibiting π–π interactions between heteroaromatic rings decreases considerably when other factors are considered, such as the geometry of the complex and the substituents. Three different orientations for the interaction between two 4-aminopyridine units were observed in the title complex using the criteria adopted by previously reported work. Nevertheless, when the supramolecular study was performed using Hirshfeld surface analysis, only one of the dimers, the one exhibiting the shortest normal distance between the planes of the interacting rings, was considered. The other interactions were confirmed by Hirshfeld surface analysis as well.

Acknowledgements

The authors acknowledge ANPCyT, CONICET (including a PhD fellowship to OCSM) and UBA (UBACYT 2014–

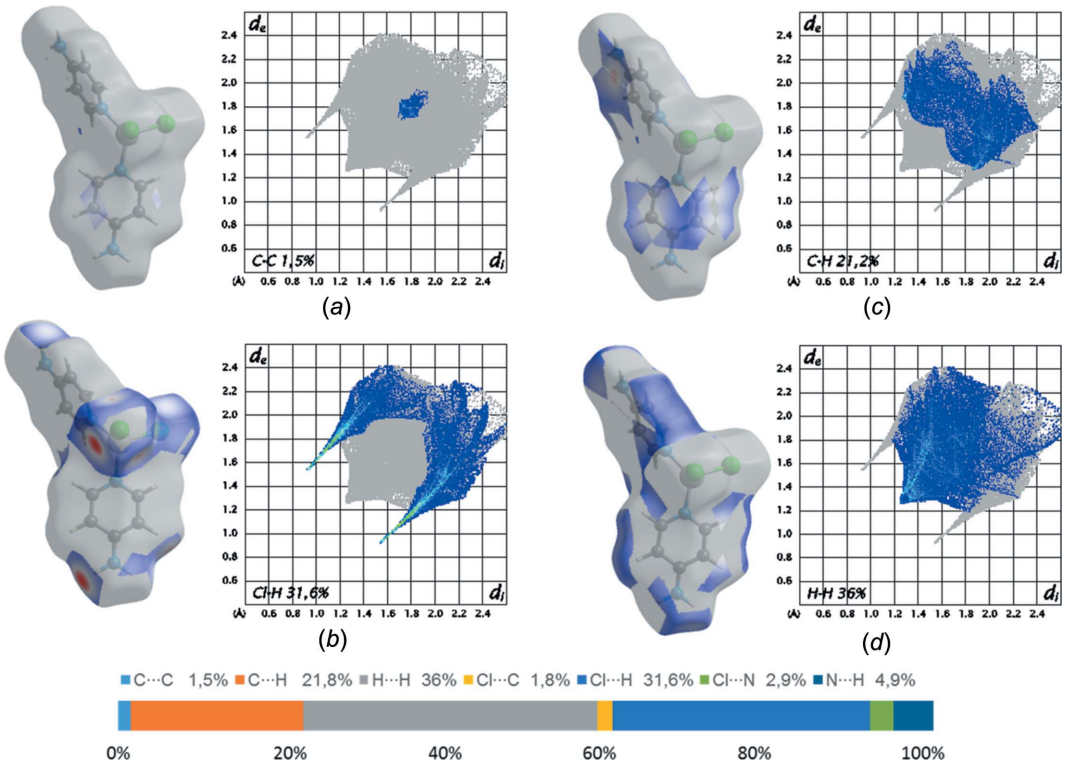

Figure 8
Percentage contributions to the HS area and fingerprint plots for $CoCl_2$(4-aminopyridine)$_2$, (I), corresponding to (*a*) C···C contacts, (*b*) C···H contacts, (*c*) Cl···H contacts and (*d*) H···H contacts. The reference for the contacts is shown at the bottom.

2017 GC) for financial support. FDS and MGR are CONICET fellows.

Funding information

Funding for this research was provided by: ANPCyT (award No. PICT 2012–1335); CONICET (award No. PIP 112 201001 00125); Universidad de Buenos Aires (award No. 20020130100642BA).

References

Agilent (2013). *CrysAlis PRO*. Agilent Technologies Ltd, Yarnton, Oxfordshire, England.
Bacchi, A., Cantoni, G., Crocco, D., Granelli, M., Pagano, P. & Pelagatti, P. (2014). *CrystEngComm*, **16**, 1001–1009.
Brown, D. J. (1985). In *The Chemistry of Heterocyclic Compounds: Pyridine Metal Complexes*. New York: Wiley.
Bruno, I. J., Cole, J. C., Edgington, P. R., Kessler, M., Macrae, C. F., McCabe, P., Pearson, J. & Taylor, R. (2002). *Acta Cryst.* B**58**, 389–397.
Bruno, I. J., Cole, J. C., Kessler, M., Luo, J., Motherwell, W. D. S., Purkis, L. H., Smith, B. R., Taylor, R., Cooper, R. I., Harris, S. E. & Orpen, A. G. (2005). *J. Chem. Inf. Comput. Sci*. **44**, 2133–2144.
Bujak, M. (2015). *Cryst. Growth Des*. **15**, 1295–1302.
Chi, Y. & Chou, P. T. (2007). *Chem. Soc. Rev*. **36**, 1421–1431.
Clarke, P. J. & Milledge, H. J. (1975). *Acta Cryst.* B**31**, 1543–1553.
Dolomanov, O. V., Bourhis, L. J., Gildea, R. J., Howard, J. A. K. & Puschmann, H. (2009). *J. Appl. Cryst.* **42**, 339–341.
Férey, G. (2008). *Chem. Soc. Rev*. **37**, 191–214.
Gill, N. S. & Nyholm, R. S. (1961). *J. Inorg. Nucl. Chem*. **18**, 88–97.
Groom, C. R., Bruno, I. J., Lightfoot, M. P. & Ward, S. C. (2016). *Acta Cryst.* B**72**, 171–179.
Hardy, J. G. (2013). . *Chem. Soc. Rev*. **42**, 7881–7899.
Hirshfeld, F. L. (1977). *Theor. Chim. Acta*, **44**, 129–138.
Janiak, C. (2000). *J. Chem. Soc. Dalton Trans*. **21**, 3885–3896.
Jian, F., Zheng, J., Zhao, P. & Li, Y. (2008). *J. Coord. Chem*. **61**, 705–714.
Lever, A. B. P. (1968). In *Inorganic Electronic Spectroscopy*. New York: Elsevier.
Ni, Y., Pan, Y.-Z., Wei, Z.-R., Cong, Q., Zhang, D., Wang, Y.-G. & Liu, X.-Y. (2013). *Inorg. Chem. Commun*. **30**, 17–20.
Nincovic, D. C., Andric, J. M. & Snezana, D. Z. (2013). *ChemPhysChem*, **14**, 237–243.
Robin, A. Y. & Fromm, K. M. (2006). *Coord. Chem. Rev*. **250**, 2127–2157.
Sheldrick, G. M. (2008). *Acta Cryst.* A**64**, 112–122.
Sheldrick, G. M. (2015). *Acta Cryst.* C**71**, 3–8.
Smith, Q. A. & Gordon, M. S. (2011). *J. Phys. Chem. A*, **115**, 4598–4609.
Spackman, M. A. & Jayatilaka, D. (2009). *CrystEngComm*, **11**, 19–32.
Spackman, M. A. & McKinnon, J. J. (2002). *CrystEngComm*, **4**, 378–392.
Spek, A. L. (2009). *Acta Cryst.* D**65**, 148–155.
Steed, J. W. & Atwood, J. L. (2009). In *Supramolecular Chemistry*, 2nd ed. Chichester: Wiley.
Sun, H.-L., Wang, Z.-M. & Gao, S. (2010). *Coord. Chem. Rev*. **254**, 1081–1100.
Teo, P. & Hor, T. S. A. (2011). *Coord. Chem. Rev*. **255**, 273–289.
Wang, W., Wnag, Y.-X. & Yang, H.-B. (2016). *Chem. Soc. Rev*. **45**, 2656–2693.
Wheeler, S. E. (2011). *J. Am. Chem. Soc*. **133**, 10262–10274.
Zhou, T., Xu, W., Li, C. & Guo, J. (2007). *Z. Kristallogr*. **222**, 249–250.

supporting information

Acta Cryst. (2017). C**73**, 399-406 [https://doi.org/10.1107/S2053229617004880]

Synthesis, crystal structure and study of the crystal packing in the complex bis-(4-aminopyridine-κN^1)dichloridocobalt(II)

Olga Carolina Sanchez Montilva, Federico Movilla, Maricel Gabriela Rodriguez and Florencia Di Salvo

Computing details

Data collection: *CrysAlis PRO* (Agilent, 2013); cell refinement: *CrysAlis PRO* (Agilent, 2013); data reduction: *CrysAlis PRO* (Agilent, 2013); program(s) used to solve structure: *SHELXS97* (Sheldrick, 2008); program(s) used to refine structure: *SHELXL2014* (Sheldrick, 2015); molecular graphics: OLEX2 (Dolomanov *et al.*, 2009); software used to prepare material for publication: OLEX2 (Dolomanov *et al.*, 2009) and *PLATON* (Spek, 2009).

Bis(4-aminopyridine-κN^1)dichloridocobalt(II)

Crystal data

$[CoCl_2(C_5H_6N_2)_2]$
M_r = 316.98
Monoclinic, *C*2/*c*
a = 8.9262 (9) Å
b = 9.9679 (10) Å
c = 14.9683 (13) Å
β = 101.825 (10)°
V = 1303.6 (2) Å^3
Z = 4
F(000) = 638
D_x = 1.603 Mg m^{-3}
Mo *Kα* radiation, *λ* = 0.71073 Å
Cell parameters from 655 reflections
θ = 4.3–23.4°
μ = 1.66 mm^{-1}
T = 293 K
Prism, blue
0.63 × 0.12 × 0.05 mm

Data collection

Xcalibur, Eos, Gemini diffractometer
Radiation source: Enhance (Mo) X-ray Source
Graphite monochromator
Detector resolution: 16.1158 pixels mm^{-1}
ω scans
Absorption correction: multi-scan (CrysAlis PRO; Agilent, 2013)
T_{min} = 0.349, T_{max} = 1.000
4351 measured reflections
1515 independent reflections
790 reflections with $I > 2\sigma(I)$
R_{int} = 0.099
θ_{max} = 28.8°, θ_{min} = 3.8°
h = −11→12
k = −11→12
l = −19→20

Refinement

Refinement on F^2
Least-squares matrix: full
$R[F^2 > 2\sigma(F^2)]$ = 0.062
$wR(F^2)$ = 0.143
S = 1.01
1515 reflections
81 parameters
0 restraints
Hydrogen site location: inferred from neighbouring sites
H atoms treated by a mixture of independent and constrained refinement
$w = 1/[\sigma^2(F_o^2) + (0.0291P)^2]$ where $P = (F_o^2 + 2F_c^2)/3$

$(\Delta/\sigma)_{max} < 0.001$
$\Delta\rho_{max} = 0.48$ e Å^{-3}
$\Delta\rho_{min} = -0.37$ e Å^{-3}

Special details

Geometry. All esds (except the esd in the dihedral angle between two l.s. planes) are estimated using the full covariance matrix. The cell esds are taken into account individually in the estimation of esds in distances, angles and torsion angles; correlations between esds in cell parameters are only used when they are defined by crystal symmetry. An approximate (isotropic) treatment of cell esds is used for estimating esds involving l.s. planes.

Fractional atomic coordinates and isotropic or equivalent isotropic displacement parameters (Å^2)

	x	*y*	*z*	U_{iso}*/U_{eq}	Occ. (<1)
Co1	0.5000	0.57032 (10)	0.7500	0.0445 (4)	0.973 (5)
Cl1	0.28833 (18)	0.43946 (15)	0.71750 (9)	0.0653 (7)	0.977 (6)
N1	0.5120 (5)	0.6761 (4)	0.6377 (3)	0.0492 (12)	
N2	0.4901 (7)	0.8335 (4)	0.3784 (3)	0.0805 (18)	
H2A	0.5401	0.7964	0.3416	0.097*	
H2B	0.4343	0.9029	0.3612	0.097*	
C5	0.4266 (6)	0.7858 (5)	0.6082 (4)	0.0510 (14)	
H5	0.3705	0.8250	0.6473	0.061*	
C1	0.5911 (7)	0.6233 (5)	0.5793 (4)	0.0603 (17)	
H1	0.6527	0.5492	0.5983	0.072*	
C2	0.5866 (8)	0.6718 (6)	0.4937 (4)	0.0663 (18)	
H2	0.6430	0.6298	0.4559	0.080*	
C3	0.4990 (7)	0.7829 (5)	0.4627 (3)	0.0559 (15)	
C4	0.4186 (6)	0.8418 (5)	0.5245 (3)	0.0537 (15)	
H4	0.3604	0.9187	0.5081	0.064*	

Atomic displacement parameters (Å^2)

	U^{11}	U^{22}	U^{33}	U^{12}	U^{13}	U^{23}
Co1	0.0407 (7)	0.0566 (8)	0.0380 (6)	0.000	0.0122 (4)	0.000
Cl1	0.0595 (11)	0.0848 (12)	0.0534 (9)	−0.0247 (9)	0.0156 (7)	−0.0028 (7)
N1	0.053 (3)	0.051 (3)	0.048 (2)	−0.009 (2)	0.021 (2)	−0.007 (2)
N2	0.127 (5)	0.067 (3)	0.047 (3)	0.005 (3)	0.019 (3)	0.009 (2)
C5	0.043 (3)	0.055 (3)	0.059 (3)	−0.005 (3)	0.021 (3)	−0.007 (3)
C1	0.074 (4)	0.055 (4)	0.060 (3)	0.007 (3)	0.034 (3)	0.005 (3)
C2	0.093 (5)	0.055 (4)	0.061 (4)	0.000 (3)	0.041 (4)	−0.006 (3)
C3	0.070 (4)	0.055 (3)	0.045 (3)	−0.018 (3)	0.017 (3)	−0.002 (3)
C4	0.052 (4)	0.054 (3)	0.054 (3)	0.001 (3)	0.007 (3)	0.005 (3)

Geometric parameters (Å, º)

Co1—Cl1^{i}	2.2652 (15)	C5—H5	0.9300
Co1—Cl1	2.2653 (15)	C5—C4	1.360 (7)
Co1—N1	2.006 (4)	C1—H1	0.9300
Co1—N1^{i}	2.006 (4)	C1—C2	1.363 (7)
N1—C5	1.354 (6)	C2—H2	0.9300
N1—C1	1.339 (6)	C2—C3	1.380 (7)

N2—H2A	0.8600	C3—C4	1.410 (7)
N2—H2B	0.8600	C4—H4	0.9300
N2—C3	1.346 (6)		

Cl1^{i}—Co1—Cl1	109.68 (9)	C4—C5—H5	118.3
N1—Co1—Cl1^{i}	107.29 (13)	N1—C1—H1	118.1
N1—Co1—Cl1	107.96 (13)	N1—C1—C2	123.8 (5)
N1^{i}—Co1—Cl1^{i}	107.96 (13)	C2—C1—H1	118.1
N1^{i}—Co1—Cl1	107.29 (14)	C1—C2—H2	119.8
N1—Co1—N1^{i}	116.6 (2)	C1—C2—C3	120.4 (5)
C5—N1—Co1	125.1 (3)	C3—C2—H2	119.8
C1—N1—Co1	117.8 (4)	N2—C3—C2	122.4 (5)
C1—N1—C5	116.2 (4)	N2—C3—C4	121.3 (6)
H2A—N2—H2B	120.0	C2—C3—C4	116.3 (5)
C3—N2—H2A	120.0	C5—C4—C3	119.8 (5)
C3—N2—H2B	120.0	C5—C4—H4	120.1
N1—C5—H5	118.3	C3—C4—H4	120.1
N1—C5—C4	123.4 (5)		

Co1—N1—C5—C4	−168.6 (4)	C5—N1—C1—C2	−1.5 (9)
Co1—N1—C1—C2	168.0 (5)	C1—N1—C5—C4	0.1 (8)
N1—C5—C4—C3	1.7 (8)	C1—C2—C3—N2	−179.4 (5)
N1—C1—C2—C3	1.0 (10)	C1—C2—C3—C4	0.9 (9)
N2—C3—C4—C5	178.1 (5)	C2—C3—C4—C5	−2.1 (8)

Symmetry code: (i) −*x*+1, *y*, −*z*+3/2.

Hydrogen-bond geometry (Å, º)

D—H···*A*	*D*—H	H···*A*	*D*···*A*	*D*—H···*A*
C5—H5···Cl1^{ii}	0.93 (1)	2.93 (1)	3.644 (6)	176 (1)
C2—H2···Cl1^{iii}	0.93 (1)	2.87 (1)	3.727 (6)	154 (1)
N2—H2b···Cl1^{iv}	0.86 (1)	2.62 (1)	3.447 (6)	163 (1)

Symmetry codes: (ii) −*x*+1/2, *y*+1/2, −*z*+3/2; (iii) −*x*+1, −*y*+1, −*z*+1; (iv) −*x*+1/2, −*y*+3/2, −*z*+1.